ELSEVIER

9 August 1996

Chemical Physics Letters 258 (1996) 53–62

CHEMICAL PHYSICS LETTERS

$\pi-\pi^*$ vibronic spectrum of ethylene from ab initio calculations of the Franck–Condon factors

Alexander M. Mebel, Yit-Tsong Chen, Sheng-Hsien Lin

Institute of Atomic and Molecular Sciences, Academia Sinica, P.O. Box 23-166, Taipei 10764, Taiwan, ROC
Department of Chemistry, National Taiwan University, Taipei 106, Taiwan, ROC

Received 15 April 1996; in final form 27 May 1996

Abstract

The vibronic spectrum of ethylene corresponding to the $\pi-\pi^*$ N–V excitation has been studied using various ab initio methods. The vertical and adiabatic excitation energies, 8.1 and 5.6 eV, respectively, obtained at the highest level of theory, MRCI, are in close agreement with experiment and the best theoretical results. The ab initio calculation of Franck–Condon factors, taking into account distortion, displacement and normal mode mixing (up to four), allowed the interpretation of major features of the observed spectrum and confirmed that the $\pi-\pi^*$ transition is responsible for the broad continuous distribution underlying the distinct Rydberg bands.

1. Introduction

Vibronic spectra of ethylene in the region of 6–8 eV have been a subject of numerous experimental [1–3] and theoretical [4–12] studies but its interpretation remains controversial. The traditional assignment attributes the prominent structure which begins at 57338 cm^{-1} to a π–3s Rydberg excitation to a $^1B_{3u}$ state and the broad underlying continuum to a $\pi-\pi^*$ N–V excitation to a $^1B_{1u}$ state. Recently, Ryu and Hudson [12] proposed a new interpretation of the entire spectrum in the 6–8 eV region based on the spectral intensity calculations for the intersecting N–V ($^1B_{1u}$) and π–3p_y ($^1B_{1g}$) surfaces. They argued that the continuos distribution that underlies the distinct Rydberg bands cannot be the N–V transition because this would require a large C–C geometry change due to the $\pi-\pi^*$ excitation, contradicting the intensity of C=C stretching overtones observed in resonance Raman spectra [12,13].

A common feature of earlier attempts to assign the vibronic spectra of C_2H_4 is that the model potentials used for the calculations include only one torsional degree of freedom or, at most, are augmented by the C–C stretching degree of freedom. The potential energy surface of ethylene has twelve degrees of freedom and of the twelve normal coordinates four are totally symmetric within D_2 symmetry, i.e., can be displaced due to the molecule twisting. The present consideration of the vibronic spectra is based on the ab initio calculations of the potential energy surfaces for the ground and excited states of ethylene as well as of vibrational frequencies,

PII S0009-2614(96)00627-6

normal coordinates and Franck–Condon factors. The Rydberg π–3s and π–3p states will be discussed in a later publication and the present Letter is devoted only to the study of the π–π^* transition.

2. Theoretical methods

The geometries of the ground (^1A_g or ^1A within D_2 symmetry) and excited states of ethylene have been optimized using CIS [8] and CASSCF methods with the 6-311(2 +)G* basis set. The latter is the standard 6-311G* basis set with two additional diffuse sp functions on carbon with exponents of 0.0438 and 0.0131928 [9]. The active space for the CASSCF calculations included 2 π electrons distributed on 11 orbitlals. The active space includes 7 σ orbitals ($3a_g + 2b_{1u} + 1b_{3g} + 1b_{2u}$ within D_{2h} symmetry or $3a + 2b_3 + 1b_1 + 1b_2$ within D_2) and 4 π orbitals ($2b_{3u} + 2b_{2g}$ for D_{2h} or $2b_1 + 2b_2$ for D_2). The (2,11) active space had been shown [10] to be sufficient for the accurate CASPT2/CASSCF calculations of the π–π^*, π–3s, π–3p, and π–3d excited states of ethylene. We have also performed some test calculations using larger (4,12), (6,13), (8,14), and (10,15) active spaces. Vibrational frequencies and normal modes have been calculated at the RHF/6-311(2 +)G* and CASSCF(2,11)/6-311(2 +)G* levels for the ground state and the CIS/6-311(2 +)G* level for the excited state.

Vertical and adiabatic excitation energies have been refined using higher levels of theory, particularly, the equation-of-motion coupled cluster method (EOM-CCSD) [14] which has been shown [15] to be a slight modification of the symmetry-adapted-cluster configuration interaction (SAC-CI) theory originally proposed by Nakatsuji [16], with the polarization basis set (PBS) of Sadlej [17]. We also used for the calculations the multireference CI method (MRCI) with the ANO basis set [18] (4s3p2d for C, 3s2p for H) augmented with several diffuse functions for the carbon atom (s exponents: 0.012138 and 0.00422482; p exponents: 0.0080150 and 0.0028052; d exponent: 0.028512) [10], designated below as ANO(2 +). The CASSCF(2,11)/ANO(2 +) wavefunction was used as initial guess for the MRCI calculations with the (2 electrons, 7 orbitals) active space. The ab initio molecular orbital calculations were carried out employing the GAUSSIAN 94 [19], ACES-II [20], and MOLCAS-3 [21] program packages.

For the calculation of Franck–Condon factors we used the normal coordinates obtained at the CIS/6-311(2 +)G* level for the excited state and at the RHF/6-311(2 +)G* level for the ground state. The ab initio program (GAUSSIAN 94) gives the normal modes in the form of the displacement matrix $|\mathbf{L}|$ connecting the vector of the mass-weighted Cartesian coordinates $\boldsymbol{q}$ with the vector of normal coordinates $\boldsymbol{Q}$:

$$\boldsymbol{Q} = |\mathbf{L}| \cdot \boldsymbol{q}, \text{ or } Q_k = \sum_{i=1}^{3n} l_{ik} q_i, \quad \text{for } k = 1,\ldots,3n-6. \tag{1}$$

For an excited state,* *

$$\boldsymbol{Q}'|\mathbf{L}'| \cdot \boldsymbol{q} + \Delta\boldsymbol{Q} = |\mathbf{L}'| \cdot |\mathbf{L}|^{-1} \cdot \boldsymbol{Q} + \Delta\boldsymbol{Q}, \tag{2}$$

where $|\mathbf{L}'|$ is the normal mode matrix for the excited state and $\Delta\boldsymbol{Q}$ is the displacement of the oscillator from the ground to the excited state. $\Delta\boldsymbol{Q}$ is calculated as

$$\Delta\boldsymbol{Q} = |\boldsymbol{L}| \cdot \Delta\boldsymbol{q} \tag{3}$$

where $\Delta\boldsymbol{q}$ is the displacement of the mass-weighted Cartesian coordinates from the ground to the excited state. Since matrix $|\mathbf{L}|$ is unitary, Eq. (2) can be written

$$\boldsymbol{Q}' = |\boldsymbol{L}'| \cdot |\boldsymbol{L}|^{\mathrm{T}} \boldsymbol{Q} + \Delta\boldsymbol{Q} = |\mathbf{C}| \cdot \boldsymbol{Q} + \Delta\boldsymbol{Q}, \tag{4}$$

where $|\mathbf{C}|$ is a Duschinsky matrix showing rotation of the normal coordinates in the excited state.

Assuming that the potential energy surfaces are harmonic, the vibrational overlap integral is defined as

$$I_{nn'} = \langle \Psi_n(Q) | \Psi_{n'}(Q') \rangle = \int \mathrm{d}Q \Psi_n(Q) \Psi_{n'}(Q') , \tag{5}$$

and the Franck–Condon factor for the $\{n\} \rightarrow \{n'\}$ transition is $|I_{nn'}|^2$. The overlap integrals have been calculated for various different cases. For ethylene, the four-mode case of displaced, distorted and rotated surfaces will be sufficient for our purpose in this Letter. The results for this case are now given.

The excited state normal coordinates Q_{α_k} are given in terms of the ground state Q_i as

$$Q_{\alpha_k} = \sum_{i=1}^{4} C_{\alpha_k i} Q_i + \Delta Q_{\alpha_k}, \quad k = 1, \ldots, 4. \tag{6}$$

Note that the vibrational overlap integral $I_{\mathrm{a0b}\nu'}$ between the two vibronic manifolds {a0} and {bν'} can be expressed in terms of the Hermite polynomia $H_n(x)$ as

$$I_{a0b\nu'} = K_{\nu'} \left[\frac{(2\pi)^4}{AD\left(\bar{\beta}_{11} \bar{\beta}_{22} - \bar{\beta}_{12}^2 \right)} \right]^{1/2} \exp\left(G - \tfrac{1}{2} \sum_{k=1}^{4} \beta_{\alpha_k} \Delta Q_{\alpha_k} \right)$$

$$\times \sum_{n_1} \sum_{n_2} \sum_{n_3} \sum_{n_4} \sum_{n_5} \sum_{n_6} \frac{(2F_{12})^{n_1}}{n_1!} \frac{(2F_{13})^{n_2}}{n_2!} \frac{(2F_{14})^{n_3}}{n_3!} \frac{(2F_{23})^{n_4}}{n_4!} \frac{(2F_{24})^{n_5}}{n_5!} \frac{(2F_{34})^{n_6}}{n_6!}$$

$$\times \frac{E_{\alpha_1\alpha_1}^{(\nu'_{\alpha_1} - n_1 - n_2 - n_3)/2} H_{\nu'_{\alpha_1} - n_1 - n_1 - n_2 - n_3}\left(E_{\alpha_1} / \sqrt{4E_{\alpha_1\alpha_1}} \right) E_{\alpha_2\alpha_2}^{(\nu'_{\alpha_2} - n_1 - n_4 - n_5)/2} H_{\nu'_{\alpha_2} - n_1 - n_4 - n_5}\left(E_{\alpha_2} / \sqrt{4E_{\alpha_2\alpha_2}} \right)}{(-1)^{\nu'_{\alpha_1} - n_1 - n_2 - n_3} (\nu'_{\alpha_1} - n_1 - n_2 - n_3)! \, (-1)^{\nu'_{\alpha_2} - n_1 - n_2 - n_5} (\nu'_{\alpha_2} - n_1 - n_4 - n_5)!}$$

$$\times \frac{E_{\alpha_3\alpha_3}^{(\nu'_{\alpha_3} - n_2 - n_4 - n_6)/2} H_{\nu'_{\alpha_3} - n_2 - n_4 - n_6 - n_3}\left(E_{\alpha_3} / \sqrt{4E_{\alpha_3\alpha_3}} \right) E_{\alpha_4\alpha_4}^{(\nu'_{\alpha_4} - n_3 - n_5 - n_6)/2} H_{\nu'_{\alpha_4} - n_3 - n_5 - n_6}\left(E_{\alpha_4} / \sqrt{4E_{\alpha_4\alpha_4}} \right)}{(-1)^{\nu'_{\alpha_3} - n_2 - n_4 - n_6} (\nu'_{\alpha_3} - n_2 - n_4 - n_6)! \, (-1)^{\nu'_{\alpha_4} - n_3 - n_5 - n_6} (\nu'_{\alpha_4} - n_3 - n_5 - n_6)!} ,$$

where a and b denote the electronic state, while $\{\nu'_{\alpha_k}\}$ represent the vibrational states. Other symbols in Eq. (7) are defined as

$$K_{\nu'} = \left(\prod_{k=1}^{4} (-1)^{\nu'_{\alpha_k}} \nu'_{\alpha_k}! \, N_{\nu'_{\alpha_k}} \right) \prod_{i=1}^{4} N_{0_i} ; \tag{8}$$

$$N_{\nu'_{\alpha_k}} = \left(\frac{\sqrt{\beta_{\alpha_k}/\pi}}{2^{\nu'_{\alpha_k}} \nu'_{\alpha_k}!} \right), \quad N_{0_i} = (\beta_i/\pi)^{1/4}, \tag{9}$$

$$\beta_i = \frac{\omega_i}{\hbar}, \quad \beta_{\alpha_k} = \frac{\omega_{\alpha_k}}{\hbar}, \tag{10}$$

where ω denotes vibrational frequency and $\hbar$ is the Planck constant divided by 2π.

$$\bar{\beta}_{ii} = \beta_i + \sum_{k=1}^{4} \beta_{\alpha_k} C_{\alpha_k i}^2, \quad \bar{\beta}_{ij} = \sum_{k=1}^{4} \beta_{\alpha_k} C_{\alpha_k i} C_{\alpha_k j}, \tag{11}$$

$$b_i = 2 \sum_{k=1}^{4} \beta_{\alpha_k} \Delta Q_{\alpha_k} C_{\alpha_k i} ; \tag{12}$$

$$A = \left(\bar{\beta}_{33} - \frac{\bar{\beta}_{13}^2}{\bar{\beta}_{11}}\right) - \frac{\left(\bar{\beta}_{23} - \frac{\bar{\beta}_{12}\bar{\beta}_{13}}{\bar{\beta}_{11}}\right)^2}{\left(\bar{\beta}_{22} - \frac{\bar{\beta}_{12}^2}{\bar{\beta}_{11}}\right)}, \tag{13}$$

$$B = -\bar{\beta}_{34} + \frac{\bar{\beta}_{13}\bar{\beta}_{14}}{\bar{\beta}_{11}} + \frac{\left(\bar{\beta}_{23} - \frac{\bar{\beta}_{12}\bar{\beta}_{13}}{\bar{\beta}_{11}}\right)\left(\bar{\beta}_{24} - \frac{\bar{\beta}_{12}\bar{\beta}_{14}}{\bar{\beta}_{11}}\right)}{\left(\bar{\beta}_{22} - \frac{\bar{\beta}_{12}^2}{\bar{\beta}_{11}}\right)}, \tag{14}$$

$$D = \bar{\beta}_{44} - \frac{\bar{\beta}_{14}^2}{\bar{\beta}_{11}} - \frac{B^2}{A} - \frac{\left(\bar{\beta}_{24} - \frac{\bar{\beta}_{12}\bar{\beta}_{14}}{\bar{\beta}_{11}}\right)^2}{\left(\bar{\beta}_{22} - \frac{\bar{\beta}_{12}^2}{\bar{\beta}_{11}}\right)}; \tag{15}$$

$$a_{\alpha_k i} = 2\sqrt{\beta_{\alpha_k}}\, C_{\alpha_k i}, \tag{16}$$

$$C_{\alpha_k} = -a_{\alpha_k 3} + \frac{\bar{\beta}_{13}}{\bar{\beta}_{11}} a_{\alpha_k 1} + \frac{\left(\bar{\beta}_{23} - \frac{\bar{\beta}_{12}\bar{\beta}_{13}}{\bar{\beta}_{11}}\right)}{\left(\bar{\beta}_{22} - \frac{\bar{\beta}_{12}^2}{\bar{\beta}_{11}}\right)}\left(a_{\alpha_k 2} - \frac{\bar{\beta}_{12} a_{\alpha_k 1}}{2\bar{\beta}_{11}}\right), \tag{17}$$

$$\Delta C = -\frac{b_3}{2} + \frac{b_1\bar{\beta}_{13}}{2\bar{\beta}_{11}} + \frac{\left(\bar{\beta}_{23} - \frac{\bar{\beta}_{12}\bar{\beta}_{13}}{\bar{\beta}_{11}}\right)}{\left(\bar{\beta}_{22} - \frac{\bar{\beta}_{12}^2}{\bar{\beta}_{11}}\right)}\left(\frac{b_2}{2} - \frac{b_1\bar{\beta}_{12}}{2\bar{\beta}_{11}}\right), \tag{18}$$

$$E_{\alpha_k} = \frac{B}{A} C_{\alpha_k} - a_{\alpha_k 4} + \frac{\bar{\beta}_{14}}{\bar{\beta}_{11}} a_{\alpha_k 1} + \frac{\left(\bar{\beta}_{24} - \frac{\bar{\beta}_{12}\bar{\beta}_{14}}{\bar{\beta}_{11}}\right)}{\left(\bar{\beta}_{22} - \frac{\bar{\beta}_{12}^2}{\bar{\beta}_{11}}\right)}\left(a_{\alpha_k 2} - \frac{\bar{\beta}_{12} a_{\alpha_k 1}}{2\bar{\beta}_{11}}\right), \tag{19}$$

$$\Delta E = -\frac{b_4}{2} + \frac{B}{A}\Delta C + \frac{b_1\bar{\beta}_{14}}{2\bar{\beta}_{11}} + \frac{\left(\bar{\beta}_{24} - \frac{\bar{\beta}_{12}\bar{\beta}_{14}}{\bar{\beta}_{11}}\right)}{\left(\bar{\beta}_{22} - \frac{\bar{\beta}_{12}^2}{\bar{\beta}_{11}}\right)}\left(\frac{b_2}{2} - \frac{b_1\bar{\beta}_{12}}{2\bar{\beta}_{11}}\right); \tag{20}$$

$$F_{kl}=\frac{E_{\alpha_k}E_{\alpha_l}}{2D}+\frac{C_{\alpha_k}C_{\alpha_l}}{2A}+\frac{a_{\alpha_k 1}a_{\alpha_k 2}}{2\bar{\beta}_{11}}+\frac{\left(a_{\alpha_k 2}-\frac{\bar{\beta}_{12}a_{\alpha_k 1}}{\bar{\beta}_{11}}\right)\left(a_{\alpha_l 2}-\frac{\bar{\beta}_{12}a_{\alpha_l 1}}{\bar{\beta}_{11}}\right)}{\left(\bar{\beta}_{22}-\frac{\bar{\beta}_{12}^2}{2\bar{\beta}_{11}}\right)}, \tag{21}$$

$$F_{\alpha_k}=\frac{\Delta EE_{\alpha_k}}{D}+\frac{\Delta CC_{\alpha_k}}{A}+\frac{b_1 a_{\alpha_k 1}}{\bar{\beta}_{11}}+\frac{\left(\frac{b_2}{2}-\frac{b_1\bar{\beta}_{12}}{2\bar{\beta}_{11}}\right)\left(a_{\alpha_k 2}-\frac{\bar{\beta}_{12}a_{\alpha_k 1}}{\bar{\beta}_{11}}\right)}{\bar{\beta}_{22}-\frac{\bar{\beta}_{12}^2}{2\bar{\beta}_{11}}}, \tag{22}$$

$$G=\frac{\Delta E^2}{2D}+\frac{\Delta C^2}{2A}+\frac{b_1^2}{2\bar{\beta}_{11}}+\frac{\left(\frac{b_2}{2}-\frac{b_1\bar{\beta}_{12}}{2\bar{\beta}_{11}}\right)^2}{2\left(\bar{\beta}_{22}-\frac{\bar{\beta}_{12}^2}{\bar{\beta}_{11}}\right)}, \tag{23}$$

$$E_{\alpha_k\alpha_k}=1-F_{kk}, \quad \text{and } E_{\alpha_k}=2\sqrt{\beta_{\alpha_k}}\,\Delta Q_{\alpha_k}-F_{\alpha_k}. \tag{24}$$

A detailed derivation of these expressions will be given in a later publication. A number of particular cases can be obtained from the above expression of the vibrational overlap integral. For example, if a particular mode is displaced and distorted but not mixed (or rotated), then

$$Q_{\alpha_k}=Q_i+\Delta Q_{\alpha_k}, \quad \omega_{\alpha_k}\neq\omega_i. \tag{25}$$

As can be seen later, for ethylene at most four modes are mixed.

3. Results and discussion

Optimized geometries of the ground and π–π^* excited states are shown in Fig. 1. Foresman et al. [8] applied the CIS method to geometry optimization of the π–π^* excited state of ethylene. In this state, the molecule is twisted by 90° and has D_{2d} symmetry, and the ground state may no longer be represented by a

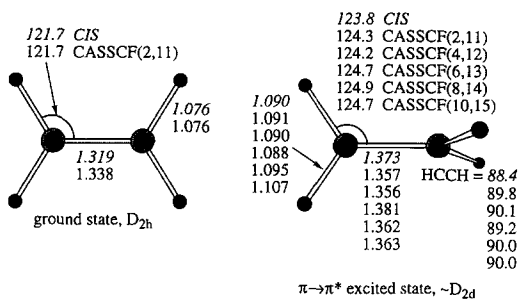

Fig. 1. Optimized geometries of the ground and $\pi-\pi^*$ excited states of ethylene (bond lengths are in Å, bond angles are in degrees). Italic numbers show geometric parameters optimized at the CIS/6-311(2+)G* level. Plain numbers are calculated at the CASSCF/6-311(2+)G* level with various active spaces. The first, second, third, fourth, and fifth plain numbers correspond to the (2,11), (4,12), (6,13), (8,14), and (10,15) active spaces, respectively.

Table 1
Vertical and adiabatic excitation energies for the $\pi \rightarrow \pi^*$ excited state of ethylene calculated at various levels of theory

Method	Ground state [a]	E_{exc} [b]	
		vertical [c]	adiabatic [d]
CIS/6-311(2 +)G *	−78.04877	7.7424 [0.51]	(5.6611)
CASSCF/6-311(2 +)G *	−78.07633	8.0816	6.5228
EOM-CCSD/PBS	−78.39040	8.0019 [0.36]	5.9109 (5.8987)
CASSCF/ANO(2 +)	−78.10057	8.1110	6.4433
MRCI/ANO(2 +)	−78.37767	8.2202	5.8182
MRCI + Dav. [e]/ANO(2 +)	−78.40554	8.1331	5.5854

[a] Total energies in hartree.
[b] Excitation energies in electron volts.
[c] In brackets: oscillator strength.
[d] At the CASSCF/6-311(2 +)G * optimized geometry and, in parentheses, at the CIS/6-311(2 +)G * optimized geometry.
[e] With Davidson correction for quadruple excitations.

single determinant because of the degeneracy of the π and π^* orbital energies. This can be avoided by using a lower symmetry, particularly D_2, for the calculations. The optimized D_2 structure does not differ substantially from D_{2d} symmetry; the deviation of the twisting angle from 90° is less than 2°. Wiberg et al. [9] and Foresman et al. [8] showed that the CIS method provides good agreement with experiment for the structure, energy and vibrational frequencies of the π–π^* state. Our results, calculated with a slightly better basis set, agree well with those of Wiberg [9] and Foresman [8]. Both CIS and CASSCF methods give for the N–V state a twisted structure of approximately D_{2d} symmetry. The other geometry changes as compared to the ground state are the elongation of the CC bond, slight lengthening of the CH bonds and opening of the CCH angles. The CC bond stretch is not large, 0.06 and 0.02 Å at the CIS and CASSCF levels, respectively. This result accords with the intensity of C=C stretching overtones in the resonance Raman spectra, as Ryu and Hudson maintain [12,13]. In order to test the sensitivity of the excited state geometry to the active space size for CASSCF, we performed calculations with (4,12), (6,13), (8,14), and (10,15) active spaces adding each time one pair of valence electrons and the corresponding orbital to the active space. The largest active space included all valence electrons, except one pair located on the fully symmetric a orbital corresponding to the σ C–H bond, distributed on 15 orbitals ($4a + 3b_3 + 4b_1 + 4b_2$ within D_2 symmetry). As seen in Fig. 1, geometrical parameters are only slightly sensitive to the active space size. Inclusion of the C–C σ bond into the (6,13) active space leads to a slight elongation of the C–C distance, from 1.36 to 1.38 Å. However, with the larger (8,14) and (10,15) active spaces, the C–C bond length decreases to 1.36 Å.

Vertical and adiabatic excitation energies, calculated at various levels of theory, are presented in Table 1. The EOM-CCSD and MRCI (with Davidson correction for quadruple excitations) methods give the vertical energy of 8.0–8.13 eV, in good agreement with earlier accurate ab initio results [4,10,11]. The EOM-CCSD calculated oscillator strength, 0.36, is in the same 0.35–0.45 range [12] with the best theoretical values. At our highest level, MRCI + Dav., the adiabatic excitation energy is 5.59 eV, while Foo and Innes [3] estimated from the experimental spectrum that the unobserved origin for the π–π^* system is situated at 5.5 eV and modeling of Siebrand, Zerbetto and Zgiersky gives the origin at 5.49 eV [7]. The MRCI method without Davidson correction and EOM-CCSD overestimates this energy by 0.2–0.3 eV as compared to the best approximation. The use of CIS and CASSCF optimized geometries for the EOM-CCSD calculations results in excitation energies different by less than 0.02 eV. The CASSCF results are 0.8–0.9 eV too high; dynamic correlation is essential to describe the adiabatic excitation energy accurately.

Calculated vibrational frequencies are collected in Table 2. Wiberg and co-workers used for scaling of the CIS frequencies of the π–π^* state the scaling factors derived from the ratios of the RHF and experimental frequencies of the ground state. All the factors are close to 0.9 and we use this number for scaling all

Table 2
Calculated vibrational frequencies (cm^{-1}) of ethylene in the ground and $\pi \rightarrow \pi^*$ excited states, scaled by 0.9 (within D_2 symmetry)

		Ground state		$\pi \rightarrow \pi^*$ excited state
		RHF/6-311(2+)G*	CASSCF/6-311(2+)G*	CIS/6-311(2+)G*
A	ν_1	2979	2979	2828
	ν_2	1640	1580	1398
	ν_3	1328	1286	1227
	ν_4	1024	977	855
B_3	ν_5	2959	2960	2798
	ν_6	1436	1435	1274
B_1	ν_7	3028	3032	2840
	ν_8	1213	1205	908
	ν_9	969	860	666
B_2	ν_{10}	3053	3059	2841
	ν_{11}	979	813	915
	ν_{12}	805	795	655

frequencies. Fig. 2 shows the normal modes of the ground state. Within D_2 symmetry, common for both states, they include 4 modes of A symmetry (ν_1–ν_4), 2 modes of B_3 symmetry (ν_5,ν_6), 3 modes of B_1 symmetry (ν_7–ν_9), and 3 modes of B_2 symmetry (ν_{10}–ν_{12}). Several frequencies change significantly from the ground to the N–V excited state, for example, HCH bending coupled with C–C stretching (ν_2, 1640 → 1398 cm^{-1}), CH_2

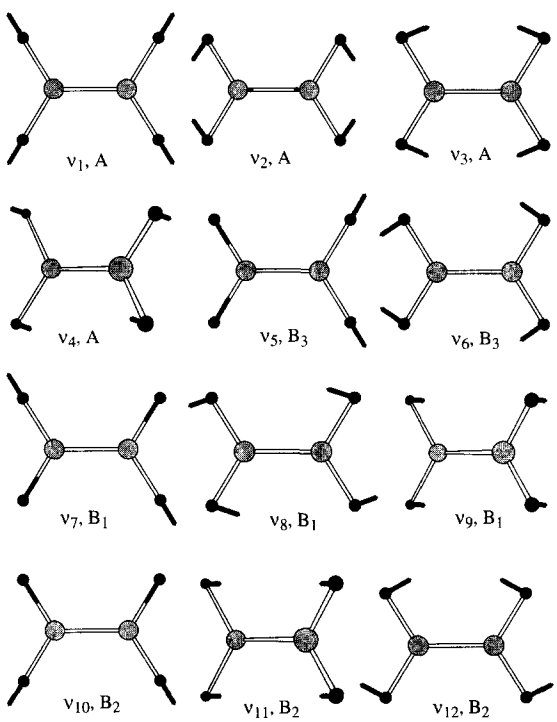

Fig. 2. Normal modes of ethylene in the ground state.

Table 3
Displacement of the oscillator (ΔQ, Å amu$^{1/2}$) and rotational Duschinsky matrix (|C|), where $Q' = |C| \cdot Q + \Delta Q$, for the $\pi \rightarrow \pi^*$ excited state of ethylene

	Q_1	Q_2	Q_3	Q_4	Q_5	Q_6	Q_7	Q_8	Q_9	Q_{10}	Q_{11}	Q_{12}
Q'_1	0.792	−0.002	−0.270	0.602	0	0	0	0	0	0	0.	0.
Q'_2	−0.183	0.814	−0.497	−0.532	0	0	0	0	0	0	0.	0.
Q'_3	0.239	−0.802	0.952	0.266	0	0	0	0	0	0	0	0.
Q'_4	−0.600	0.480	−0.180	0.720	0	0	0	0	0	0	0.	0.
Q'_5	0	0	0	0	0.796	−0.088	0	0	0	0	0	0.
Q'_6	0	0	0	0	−0.068	0.906	0	0	0	0	0	0.
Q'_7	0	0	0	0	0	0	0.802	−0.075	−0.561	0	0	0.
Q'_8	0	0	0	0	0	0	0.343	0.954	−0.320	0	0	0.
Q'_9	0	0	0	0	0	0	0.568	0.082	0.811	0	0	0.
Q'_{10}	0	0	0	0	0	0	0	0	0	0.785	0.468	−0.415
Q'_{11}	0	0	0	0	0	0	0	0	0	−0.583	0.594	−0.392
Q'_{12}	0	0	0	0	0	0	0	0	0	0.210	0.674	0.802
ΔQ [a]	0.398	0.421	0.346	1.263	0	0	0	0	0	0	0	0.
	0.416	0.469	0.286	1.273	0	0	0	0	0	0	0	0

[a] The first and second lines are calculated from CIS and CASSCF optimized geometries, respectively.

twisting (ν_4, 1024 → 855 cm^{-1}), CCH bending (ν_8, 1213 → 908 cm^{-1}), CH_2 torsion (ν_9, 969 → 666 cm^{-1}), asymmetric CH stretching (ν_{10}, 3053 → 2841 cm^{-1}), and CCH bending (ν_{12}, 805 → 655 cm^{-1}). Frequencies for the excited state are in general lower than those for the ground state, i.e., the oscillators are distorted.

Displacement of the oscillators is shown in Table 3. Upon excitation, D_2 symmetry is conserved; therefore, only totally symmetric A modes are displaced and the modes of B_1–B_3 symmetries have zero ΔQ. For all four A modes, ΔQ values are high and the highest of them, 1.26–1.27 Å (amu)$^{1/2}$, is found for the CH_2 twisting ν_4, which is not surprising because in the excited state the molecule is twisted by 90°. The calculation of the Huang–Rhys factors S for the ν_1–ν_4 modes gives values of 6.82, 3.98, 2.27, and 22.14, respectively. If we used the approach of the displaced oscillator to compute the Franck–Condon factors, the maximum would be for the $0 \rightarrow (6,3,2,22)'$ transition and its value is 6.753×10^{-4}. This peak is located as far as at 42426 cm^{-1} from the origin.

However, the four A modes are not only displaced but also rotated, that is, mixed. This is one of the reasons why the calculated ΔQ are high. The rotational matrix (Duschinsky matrix |**C**|) is shown in Table 3. After normalization, it was used for the computation of the Franck–Condon factors. Before discussing the results for the modes of A symmetry, mostly responsible for the shape of the spectrum, let us consider first the Franck–Condon factors for the other modes. The B_1–B_3 oscillators are not displaced and the structure of the spectrum is due to distortion and rotation. For instance, for B_3 modes (ν_5,ν_6), $|I_{0,0'}|^2 = 0.9852$, $|I_{0,(11)'}|^2 = 0.0108$. For the modes of B_1 symmetry (ν_7–ν_9), $|I_{0,0'}|^2 = 0.8300$, $|I_{0,(200)'}|^2 = 0.0106$, $|I_{0,(110)'}|^2 = 0.0184$, $|I_{0,(101)'}|^2 = 0.0471$, and $|I_{0,(002)'}|^2 = 0.0574$. For the B_2 modes (ν_{10}–ν_{12}), the Franck–Condon factors are similar: $|I_{0,0'}|^2 = 0.8473$, $|I_{0,(200)'}|^2 = 0.0221$, $|I_{0,(110)'}|^2 = 0.0573$, and $|I_{0,(020)'}|_2 = 0.0422$. Thus, distortion and rotation do not decrease the $|I_{0,0'}|^2$ value much with zero displacement.

Calculated spectra based on the Franck–Condon factors for the fully 12 modes are shown in Fig. 3 on (a) linear and (b) logarithmic scales. One can see that the π–π^* vibronic spectrum indeed is an underlying continuum spreading to as high an energy as 85000 cm^{-1}. The Franck–Condon factors are low; the maximal value does not exceed 2×10^{-4}. The highest peaks are located between 75000 and 80000 cm^{-1}, i.e., 30000–35000 cm^{-1} from the origin. If rotation is not taken into account, the maximum is found about 10000 cm^{-1} farther. The spectrum can be divided into several intervals. Franck–Condon factors of 10^{-4} and higher lie in the 70000–84000 cm^{-1} energy range. The values of 10^{-5}–10^{-4} are calculated for the 62000–70000 cm^{-1} range. The transitions in the 58700–62000 cm^{-1} interval have the Franck–Condon factors of 10^{-6}–10^{-5}. It

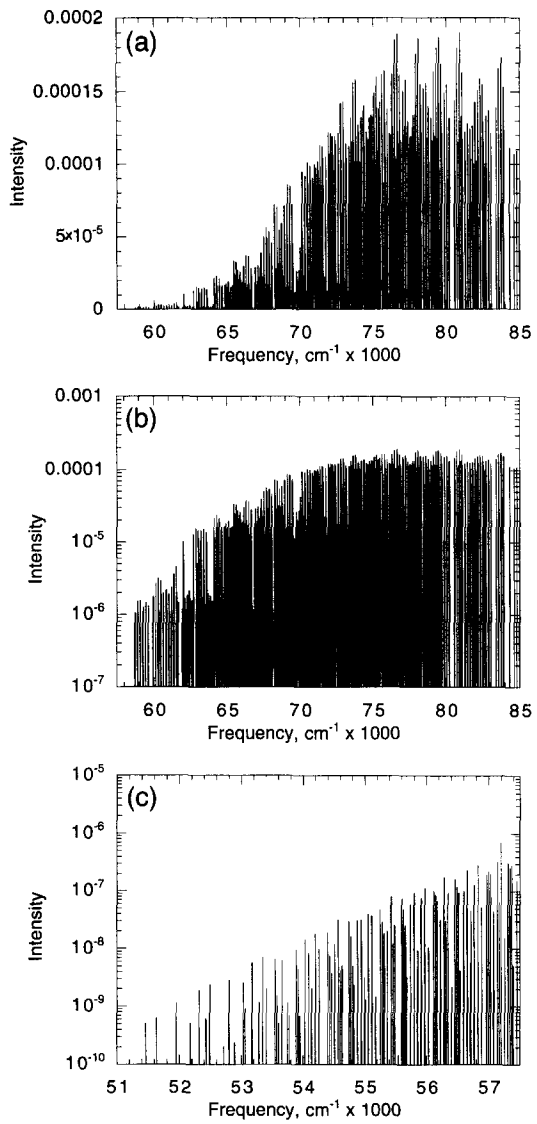

Fig. 3. Calculated vibronic spectra of ethylene for the $\pi-\pi^*$ transition: (a) on a linear scale; (b) on a logarithmic scale; (c) on a logarithmic scale in the interval 51000–57500 cm^{-1}.

should be mentioned that the vertical excitation energy is about 65600 cm^{-1}, but the highest Franck–Condon factors are found after 70000 cm^{-1}. This deviation can probably be attributed to the large rotation and displacement of the real potential for the excited state.

Fig. 3(c) shows the so called 'foot' of the vibronic spectrum of ethylene, the region of 51000–57500 cm^{-1} before the beginning of the prominent structure. Franck–Condon factors are low but the shape of the spectrum on the logarithmic scale reproduces the shape of the observed absorption spectrum [2]. Both in theory and in experiment the intensity of the peaks increases by three orders of magnitude from 51000 to 57500 cm^{-1}. The ab initio calculations of the Franck–Condon factors for the $\pi-\pi^*$ transition allowed us to interpret major

qualitative features of the observed spectrum. Our results confirm that this state is responsible for the broad continuous distribution which underlies the distinct Rydberg bands.

Acknowledgements

AMM is grateful to Academia Sinica for a fellowship at IAMS. Helpful discussion with Dr. Alexei Pakhomov is much appreciated. This work was supported in part by the National Science Council of ROC.

References

[1] M.B. Robin, Higher excited states of polyatomic molecules (Academic Press, New York, 1975; 1985) Vol. 2, p. 2; Vol. 3, p. 213.
[2] P.G. Wilkinson and R.S. Mulliken, J. Chem. Phys. 23 (1955) 1895; P.G. Wilkinson, J. Mol. Spectrosc. 6 (1961) 1.
[3] P.D. Foo and K.K. Innes, J. Chem. Phys. 60 (1974) 4582.
[4] C. Petrongolo, R.J. Buenker and S.D. Peyerimhoff, J. Chem. Phys. 76 (1982) 3655; 78 (1983) 7284.
[5] H. Nakatsuji, J. Chem. Phys. 80 (1984) 3703.
[6] M.H. Palmer, A.J. Beveridge, I.C. Walker and T. Abuain, Chem. Phys. 102 (1986) 63.
[7] W. Siebrand, F. Zerbetto and M. Zgiersky, Chem. Phys. Lett. 174 (1990) 119.
[8] J.B. Foresman, M. Head-Gordon, J.A. Pople and M.J. Frisch, J. Phys. Chem. 96 (1992) 135.
[9] K.B. Wiberg, C.M. Hadad, J.B. Foresman and W.A. Chupka, J. Phys. Chem. 96 (1992) 10756.
[10] L. Serrano-Andres, M. Merchan, I. Nebot-Gil, R. Lindh and B.O. Roos, J. Chem. Phys. 98 (1993) 3151.
[11] R. Lindh and B.O. Roos, Int. J. Quantum Chem. 35 (1989) 813.
[12] J.-S. Ryu and B.S. Hudson, Chem. Phys. Lett. 245 (1995) 448.
[13] R.J. Sension and B.S. Hudson, J. Chem. Phys. 90 (1989) 1377.
[14] J.F. Stanton and R.J. Bartlett, J. Chem. Phys. 98 (1993) 7029.
[15] H. Nakatsuji and M. Ehara, J. Chem. Phys. 101 (1994) 7658.
[16] H. Nakatsuji, Chem. Phys. Letters 59 (1978) 362; 67 (1979) 329; 67 (1979) 334; K. Hirao, J. Chem. Phys 79 (1983) 5000.
[17] A.J. Sadlej, Coll. Czech. Chem. Commun. 53 (1988) 1995; A.J. Sadlej, Theor. Chim. Acta. 79 (1991) 123.
[18] P.-O. Widmark, P.-Å. Malmqvist and B.O. Roos, Theor. Chim. Acta. 77 (1990) 291.
[19] M.J. Frisch, G.W. Trucks, H.B. Schlegel, P.M.W. Gill, B.G. Johnson, M.A. Robb, J.R. Cheeseman, T. Keith, G.A. Petersson, J.A. Montgomery, K. Raghavachari, M.A. Al-Laham, V.G. Zakrzewski, J.V. Ortiz, J.B. Foresman, J. Cioslowski, B.B. Stefanov, A. Nanayakkara, M. Challacombe, C.Y. Peng, P.Y. Ayala, W. Chen, M.W. Wong, J.L. Andres, E.S. Replogle, R. Gomperts, R.L. Martin, D.J. Fox, J.S. Binkley, D.J. Defrees, J. Baker, J.P. Stewart, M. Head-Gordon, C. Gonzalez and J.A. Pople, GAUSSIAN 94, Revision B.2, (Gaussian, Inc., Pittsburgh PA, 1995).
[20] J.F. Stanton, J. Gauss, J.D. Watts, W.J. Lauderdale and R.J. Bartlett, ACES-II, University of Florida, USA.
[21] K. Andersson, M.R.A. Blomberg, M.P. Fulscher, G. Karlstrom, V. Kello, R. Lindh, P.-Å. Malmqvist, J. Noga, J. Olsen, B.O. Roos, A.J. Sadlej, P.E.M. Siegbahn, M. Urban and P.-O. Widmark, MOLCAS-3, University of Lund, Sweden.